Neuron, Volume 73

Supplemental Information

Only Coherent Spiking in Posterior Parietal Cortex Coordinates Looking and Reaching

Heather L. Dean, Maureen A. Hagan, and Bijan Pesaran

Supplemental Data

We recorded spiking and LFP activity from 105 sites in area LIP (74 in Monkey H; 31 in Monkey J), 135 sites in PRR (53 in Monkey H; 82 in Monkey J) and 54 sites in visual area 3 (V3d; 54 in Monkey J; **Fig 3a, Fig S1**).

Classification of RT Better for Coherent than Noncoherent Cells

As described in the Methods, we used Fisher's linear discriminant analysis to decode whether single trials were from the fastest or slowest RTs in reach and saccade trials in the preferred direction. After ranking the RT selectivity of each cell using an ANOVA, we decoded the identity (fast or slow RT) of each trial on an increasing subset of cells from two to 25 and computed the probability of correct classification. Cells were ranked according to the results of the ANOVA and added to the test set in that order. Here, we present the data across increasing subsets of cells (**Fig S2**). For most dataset sizes, coherent cells (solid lines) more accurately predicted RT than not coherent cells (dashed lines). Coherent cells best predicted reach reaction time (RRT, green lines) and saccade reaction time (SRT, red lines) during a coordinated movement. The RT of saccades made alone (black lines) was not significantly well predicted by either coherent or not coherent cells.

Beta Band but not Gamma Band LFP Power in area LIP Is Influenced by Movement Type

Immediately after a spatial cue is presented in the preferred location for that site, LFP power in area LIP is directionally selective at 45 Hz, showing greater selectivity at that frequency and above for movements in the preferred direction (**Fig S3a,b**). During the delay period that follows, selectivity at frequencies above 100 Hz drops off but remains strongest at 30-50 Hz. Gamma-band LFP power is similarly spatially selective before a reach and saccade.

LFP power at 15 Hz is directionally selective but shows a different response than power at 45 Hz and depends on whether a coordinated reach is made with a saccade ($p<<0.05$, rank-sum test, **Fig S3c,** see **Fig 7a**). Average 15 Hz directional selectivity across the population is influenced by reaches, differing for reaches and saccades versus saccades alone in the late delay ($p<<0.05$, t-test). Consequently, selectivity of beta band LFP power in area LIP before saccades changes when a coordinated reach movement is also made. Activity at 45 Hz, on the other hand, does not differ significantly for saccades made with or without a reach ($p = 0.74$, rank-sum test, **Fig S3d,** see **Fig 7b**)

Beta Band Directional Tuning Specific Is to Reaching Areas

To establish the specificity of LFP activity in area LIP before coordinated reach-and-saccade movements, we also recorded LFP activity at 135 sites in PRR (53 in Monkey H; 82 in Monkey J, **Fig S4**) and another 54 sites in V3d in Monkey J (**Fig S5**).

Examining the spatial tuning of PRR activity for each frequency and time during trials involving a reach and saccade or a saccade alone reveals similarities and differences with activity in area LIP (**Fig S4**). During the memory period before movement, directional selectivity of LFP activity in PRR is most pronounced in activity around 15 Hz. In addition, similar to area LIP, selectivity of memory period activity around 15 Hz depends on whether a reach is made with a saccade ($p<<0.05$, rank-sum test, **Fig S4a,b,** see **Fig 8c**). As in area LIP, directional selectivity associated with a reach is more often associated with a reduction in power before movements to the preferred direction (**Fig S4c**). Thus, movement specific directionally-tuned activity at 15 Hz is present in PRR as well as in area LIP. As in area LIP, gamma-band activity in PRR does not differ significantly for saccades made with or without a reach ($p=0.33$, rank-sum test, **Fig S4d**, see **Fig 8d**).

LFP activity in V3d, which is part of the dorsal stream that projects to posterior parietal cortex, contains a different pattern of selectivity. We recorded from 54 sites in V3d and limited our analysis to the 36 sites that were significantly visually responsive at 75-175 Hz (peak in our z-score direction selectivity) just after cue onset when the cue was presented in the visual hemifield contralateral to the recording hemisphere ($p<0.05$, **Fig S5a,b**). These sites show less directional selectivity at both beta (**Fig S5c**) and gamma frequencies (**Fig S5d**). As in parietal areas, there is no significant difference at 45 Hz for saccades made with or without a reach during the delay ($p=0.24$, rank-sum test, **Fig 8e**). The directional selectivity at 15 Hz also does not differ for saccades made with or without a reach ($p=0.22$, rank-sum test, **Fig 8f**). Therefore, directional and movement type selectivity is not a general feature of LFP activity in cortical regions and is specific to beta band LFP activity in area LIP and PRR.

Supplemental Experimental Procedures

Neural Recording Protocol

Cells were first isolated and, if stable, recorded during the center-out reach-and-saccade task to map the response field. After these initial experiments, if there was a significant response to the task, recordings proceeded as described above for targets in the preferred and null directions. Occasionally, cells were acquired on additional electrodes and recorded despite the fact they had no task response or cells were lost during a recording. All cells that were recorded for a minimum of 20 trials per condition were included in the database regardless of task response.

Preprocessing of Neural Recordings

Spike events were extracted and classified from the broad-band activity using custom Matlab code (The Mathworks, MA) during the recording session and resorted off-line. Single-unit activity was generated by band-pass filtering the signal from 0.3 to 6.6 kHz, extracting waveforms that crossed a threshold (typically 3.5 standard deviations of the band-pass filtered activity), upsampling 4x and aligning waveforms to the peak negativity or positivity. To account for non-stationarity in the recordings, spike classification was done on a 100 s moving window and clusters were tracked across windows. Occasionally there were periods when clusters were not isolated. Trials during those periods were marked, and this data was not subject to further analysis.

LFP activity was generated by low-pass filtering the raw, broad-band recording at 300 Hz and decimating the signal to 1 kHz. Filtered LFP data can be seen in Figures **3bi** and **3ci**. All spectral analysis was performed using multitaper spectral analyses methods (Mitra and Pesaran, 1999). The LFP spectrum was calculated on a 0.5 s analysis window with ±5 Hz

frequency smoothing. The LFP spectrogram was calculated by stepping the analysis window 50 ms between estimates.

Spectral density was calculated using Parceval's Theorem. We scaled the spectrum by the power in the mean LFP (σ^2) divided by the mean energy in the spectrum. To show change from baseline for spectral signals, the spectrum at a given time and frequency was divided by activity at that frequency in our baseline epoch, defined as the 0.5 s before target onset. We measured the mean noise floor in the recording room with a 1 MOhm electrode in saline and found the integrated spectral power between 1 and 300 Hz was 1.8 μV^2, establishing a noise floor well below the level of the signals reported here.

Matching the Firing Rate

In the **Results**, we argue that the definition of coherent spiking activity is not simply due to high firing rate. Our reasoning is that if a cell is not coherently active with a field but has a high firing rate, we are not more likely to report that the coherence is significant than if the firing rate is low. We have confirmed this claim numerically. We take a session of LFP recordings and then generate 1000 Poisson distributed spike trains with different firing rates ranging from 5 spikes/s to 100 spikes/s which represents spiking activity that is uncorrelated with the LFP. We then measure how frequently we determine that spike-field coherence was significant using a non-parametric permutation test described in the **Methods**. We find that the frequency with which we detected spike-field coherence was 5%, in line with our statistical significance threshold, and the proportion of false positives was the same for low and high firing rates. This result is in line with the results reported by (Maris et al. 2007) when they compared significance for different numbers of trials and found that the non-parametric permutation test controls the false alarm rate.

Figure S1 (Pesaran)

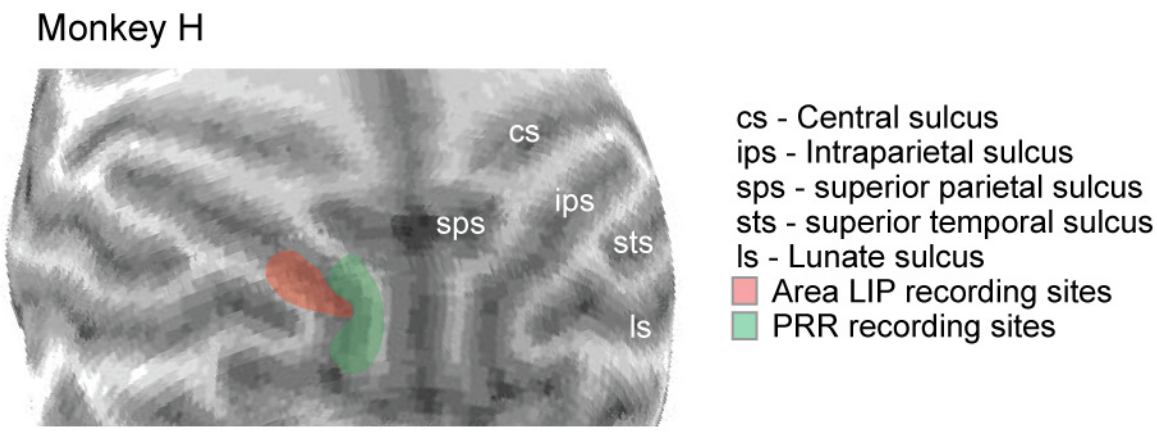

Figure S1. Recording Sites in Monkey H, Related to Figure 3

Structural magnetic resonance image. cs -Central sulcus; ips -Intraparietal sulcus; sps - superior parietal sulcus; sts - superior temporal sulcus; ls -Lunate sulcus.

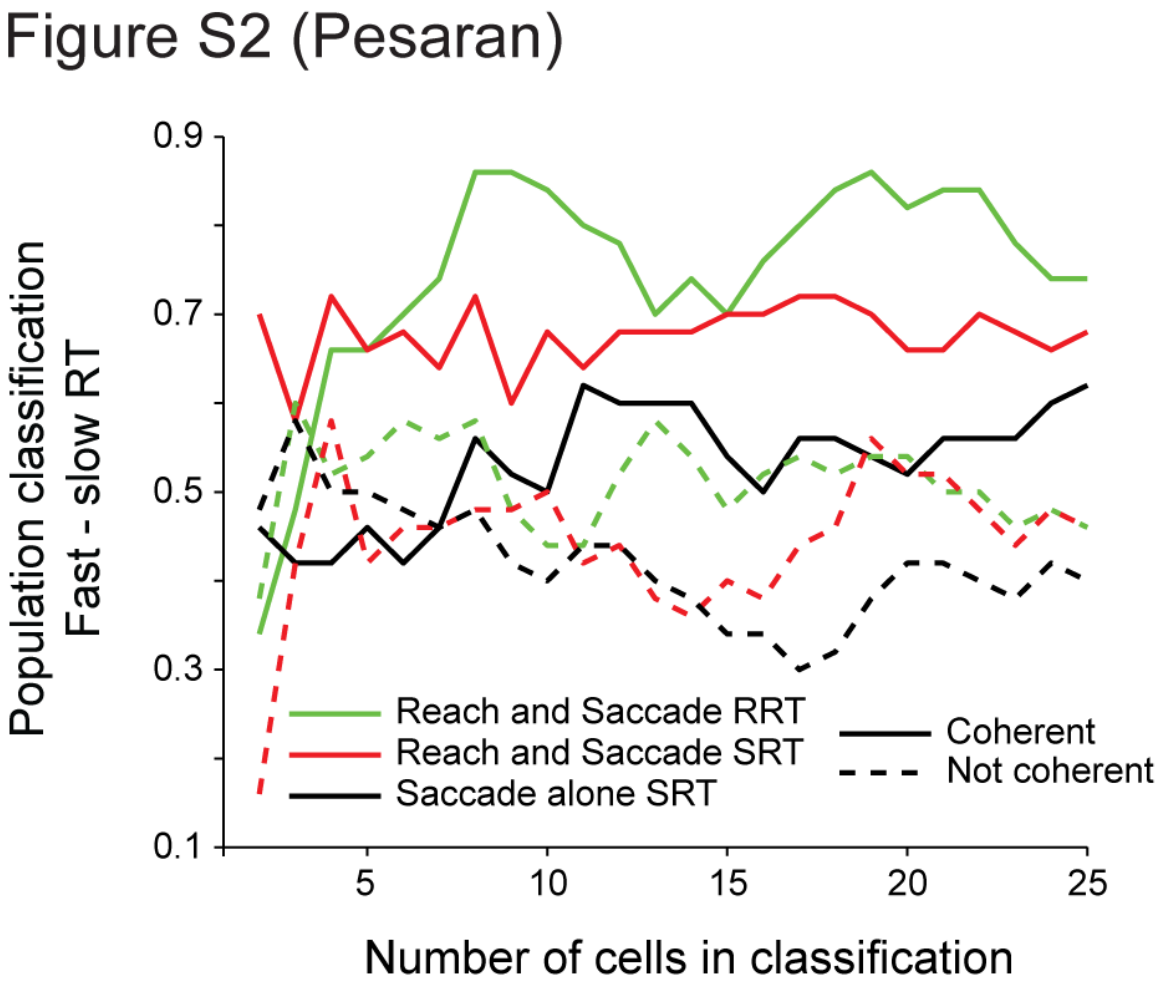

Figure S2. Performance Curves, Related to Figure 5

Performance curves for classification of coordinated RRT (green), coordinated SRT (red) and saccade alone SRT (black). Analysis with significantly coherent cells (solid lines) and analysis with not significantly coherent cells (dashed lines).

Figure S3 (Pesaran)

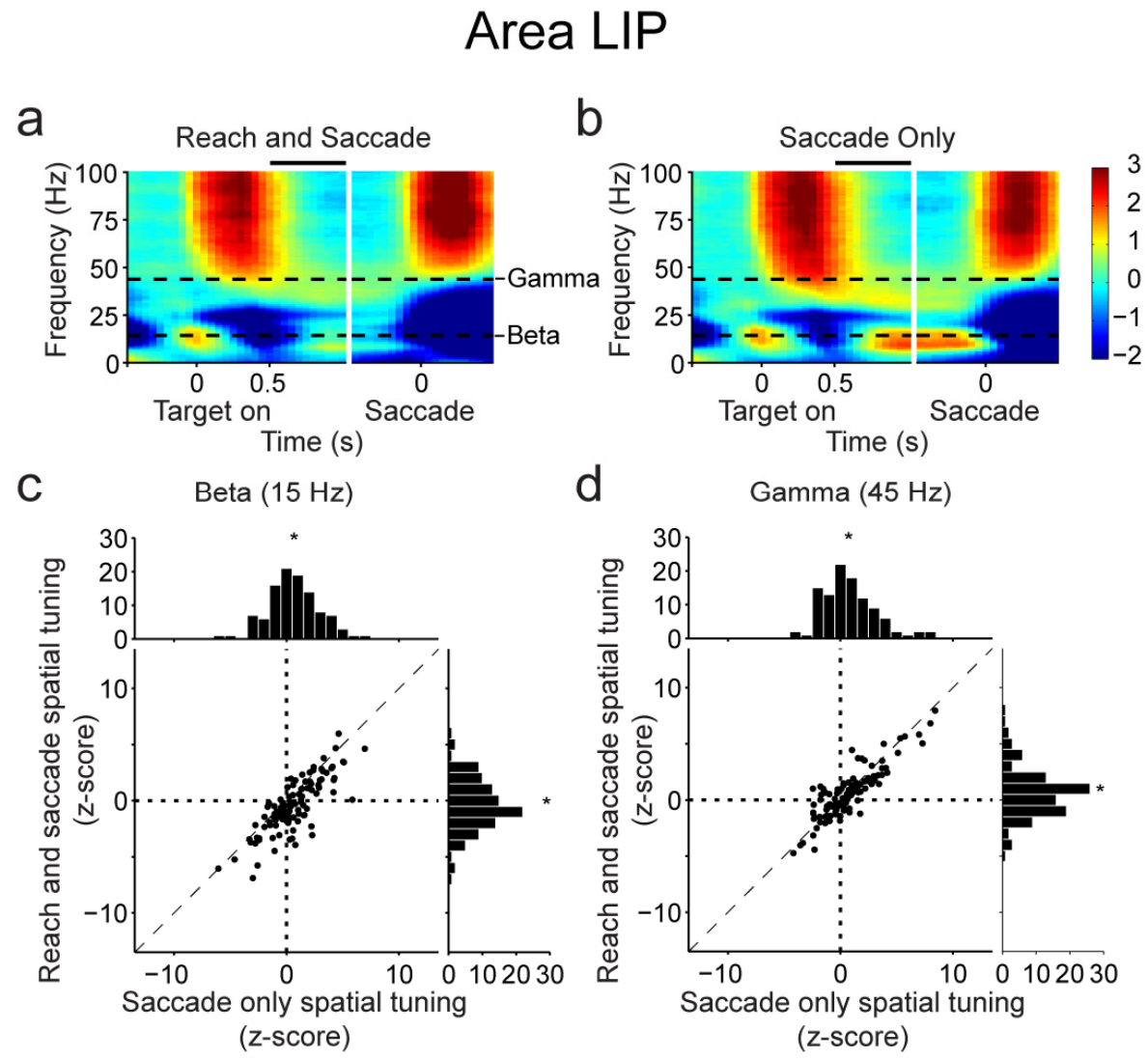

Figure S3. Area LIP Population Analysis, Related to Figure 8

(a) Average z-score aligned on target onset and on saccade start during the Reach and Saccade task.

(b) Same as **a** during the Saccade task. Horizontal black lines above data indicate time of scatter plots in **c** and **d**. Gray indicates 95% confidence interval.

(c) Distribution of z-scores for each task at 15 Hz.

(d) Same as **c** at 45 Hz.

Figure S4 (Pesaran)

PRR

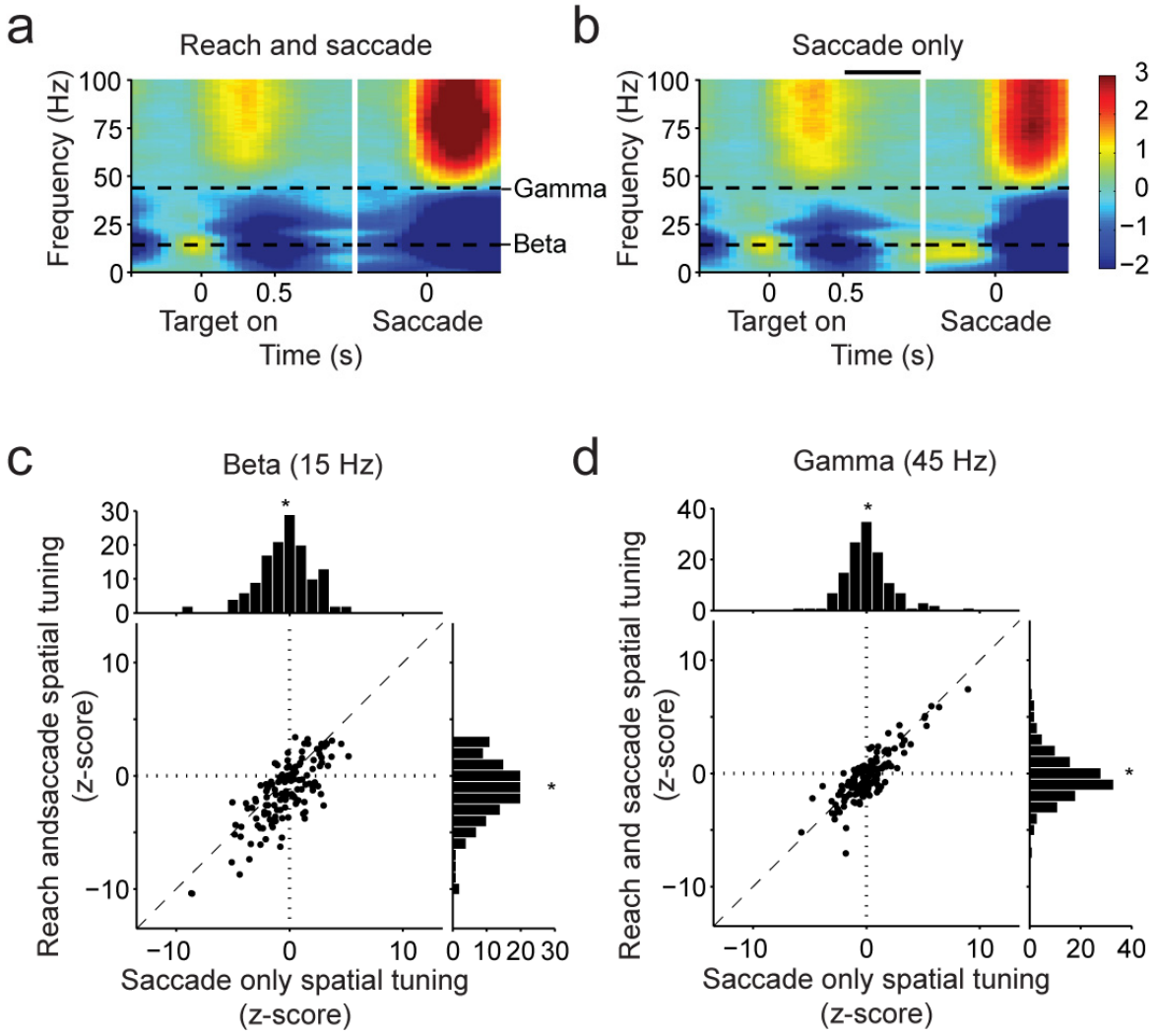

Figure S4. PRR Population Analysis, Related to Figure 8

(a) Average z-score aligned on target onset and on saccade start during the Reach and Saccade task.

(b) Same as **a** during the Saccade task. Horizontal black lines above data indicate time of scatter plots in **c** and **d**. Gray indicates 95% confidence interval.

(c) Distribution of z-scores for each task at 15 Hz.

(d) Same as **c** at 45 Hz.

Figure S5 (Pesaran)

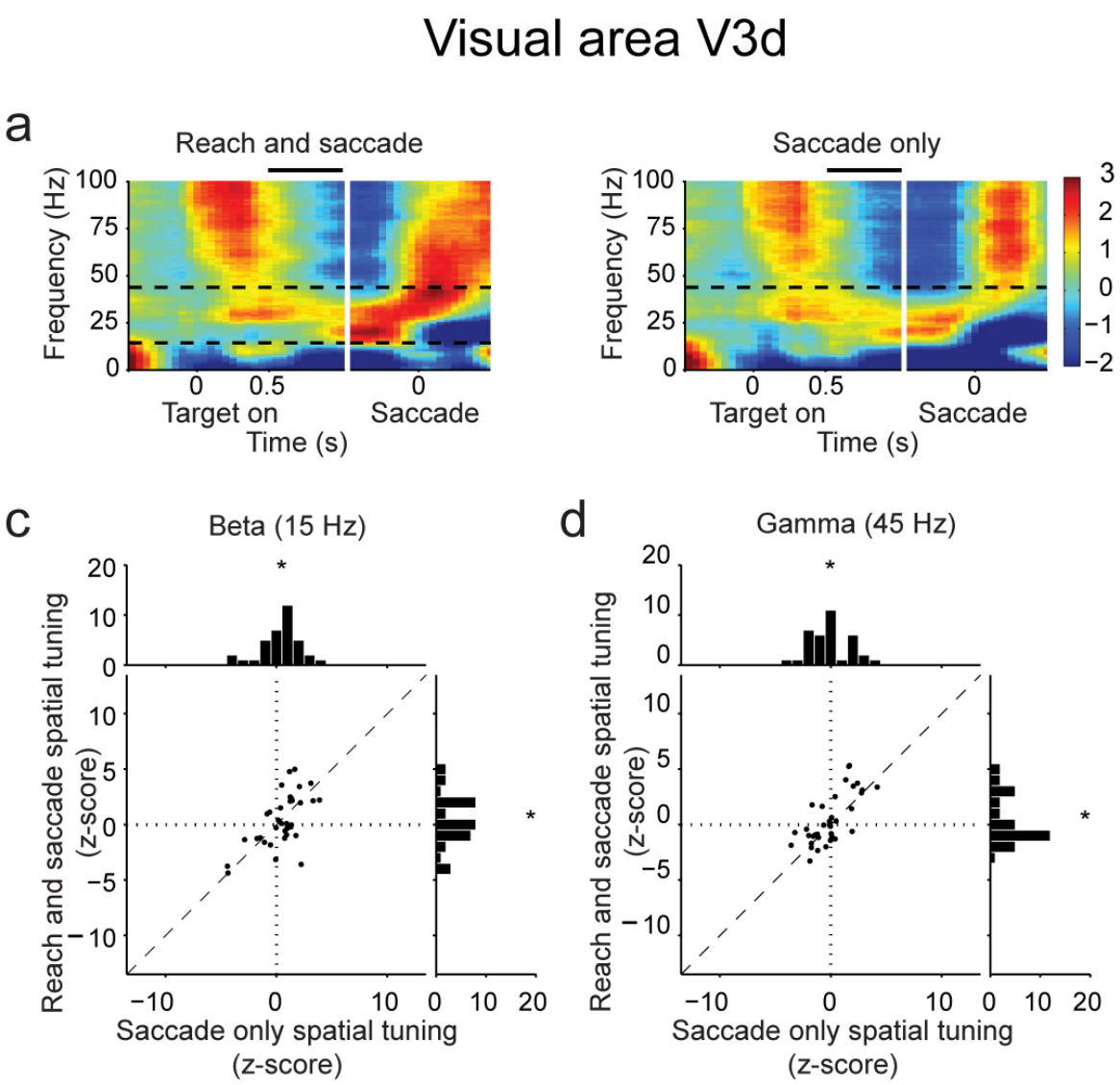

Figure S5. Visual Area 3D Population Analysis, Related to Figure 8

(a) Average z-score aligned on target onset and on saccade start during the Reach and Saccade task.

(b) Same as **a** during the Saccade task. Horizontal black lines above data indicate time of scatter plots in **c** and **d**. Gray indicates 95% confidence interval.

(c) Distribution of z-scores for each task at 15 Hz.

(d) Same as **c** at 45 Hz.